CONF-9507160--3
SAND95-2482C

Development of Backscattered Electron Kikuchi Patterns for Phase Identification in the SEM

J. R. Michael and R. P. Goehner
Sandia National Laboratories
Albuquerque, NM 87185-1405

Abstract

This paper describes the use of backscattered electron Kikuchi patterns (BEKP) for phase identification in the scanning electron microscope (SEM). The origin of BEKP is described followed by a discussion of detectors capable of recording high quality patterns. In this study a new detector based on charge coupled device technology is described. Identification of unknown phases is demonstrated on prepared and as received sample surfaces. Identification through a combination of energy dispersive x-ray spectrometry (EDS) and BEKP of a Laves phase in a weld in an alloy of Fe-Co-Ni-Cr-Nb and the identification of $Pb_2Ru_2O_{6.5}$ crystals on PZT is demonstrated. Crystallographic phase analysis of micron sized phases in the SEM is a powerful new tool for materials characterization.

THE IDENTIFICATION OF UNKNOWN MICRON-SIZED PHASES in the SEM has been limited by the lack of a robust and simple way to obtain crystallographic information about the unknown while observing the microstructure of the specimen. A variety of techniques are available that can provide some information about the identity of unknown phases. For example, EDS is of some use but obviously cannot distinguish between phases with similar compositions but different crystal structures (an example of this is TiO_2 that has two tetragonal forms with different atomic arrangements and an orthorhombic form). Electron channeling patterns (ECP) in the SEM can provide appropriate information about the crystallography of the unknown, but the technique is limited by spatial resolution and sensitivity to plastic strain and is not applicable to rough surfaces. Other techniques can provide the required information but have significant disadvantages when compared to BEKP. Selected area electron diffraction in the transmission electron microscope (TEM) can provide crystallographic information from micron-sized regions of the specimen, but TEM requires electron transparent thin specimens to be produced which is time consuming and can be very difficult. BEKP in the SEM can provide crystallographic information from sub-micron sized areas with little or no difficult specimen preparation.

Backscattered electron Kikuchi patterns were first observed over 40 years ago before the development of the SEM (1). The patterns were recorded on photographic film inside an evacuated chamber. It was not until the 1970's that a suitable detector system was attached to an SEM and BEKPs observed (2). At this time the authors recognized that the patterns could be used to determine accurate crystallographic orientations of sub-micron sized crystals (3). More recently, the technique has been highly developed to provide accurate crystallographic orientation of grains in polycrystalline materials. This information is then used to determine the microtexture of the specimen (4,5).

BEKP's have been used to identify crystal symmetry elements and crystallographic point groups. This work showed that 27 of the 32 possible point groups could be identified using BEKP (6-10). The pattern quality required for these studies dictated that photographic film be used to record the images. The recording of BEKP on film requires that a suitable film transport mechanism be added to the SEM, although recently a 35 mm camera body has been used inside the vacuum of an SEM for this purpose. Although, photographic recording of BEKP is possible, it is not a real time technique suitable for on-line phase identification.

The development of a camera for BEKP recording that is based on CCD (charge coupled device) technology has enabled phase identification to be performed rapidly in the SEM using BEKP (11). This paper will briefly discuss the origin of the patterns and then will describe how BEKPs can be utilized to provide crystallographic phase identification of sub-micron areas.

Origin of Backscattered Electron Kikuchi Patterns

Backscattered electron Kikuchi patterns are obtained by illuminating a highly tilted specimen with a stationary electron beam. The beam electrons are elastically and inelastically scattered within the specimen with some of the electrons scattered out of the specimen. These backscattered electrons form the diffraction pattern. There are currently two mechanisms used to describe the pattern formation. In the first description, Kikuchi patterns are formed by the elastic scattering (diffraction) of previously inelastically scattered electrons. Some of the inelastically scattered electrons satisfy the Bragg condition for diffraction and are diffracted into cones of intensity which form the pattern when imaged with a suitable detector (1). An alternative description of the pattern formation requires one high angle scattering event that results in an electron exiting the specimen. The channeling of these electrons by the crystallographic planes of the specimen results in the formation of the cones of intensity in a matter analogous to the channeling of electrons in electron channeling patterns (12). Fortunately, we do not require a detailed understanding of the physics of electron scattering to use these patterns for phase identification in the SEM.

The specimen must be tilted to a high angle (typically 70°) with respect to the electron beam for two reasons as shown in Figure 1. Figure 1 is a plot of the energy distribution of backscattered electrons from Ni for a beam voltage of 30 kV for an electron beam normal to the specimen surface and for a beam that is 70° from the surface normal. The advantages of utilizing a tilted specimen can be shown by comparing the data for the normal incidence and the tilted beam. First, the number of backscattered electrons is greatly increased by tilting the sample. This results in a much greater signal that permits the patterns to be observed.

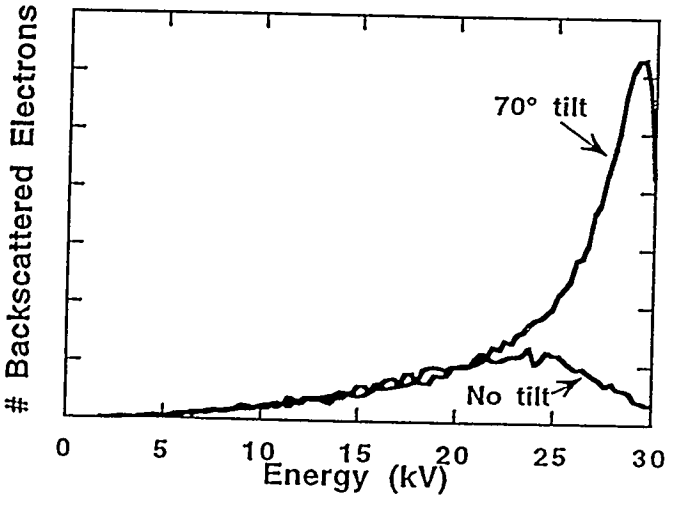

Fig. 1 Plot of the energy distribution for electrons backscattered from a tilted and a flat sample in the SEM.

Secondly, when the specimen is tilted to high angles, the backscattered electrons do not penetrate as deeply into the specimen as for the untilted specimen. Thus, the backscattered electrons lose a much smaller amount of energy on average resulting in a sharp peak in the backscattered electron energy distribution that is very close to the initial beam energy. The electrons in this sharp peak contribute to the diffraction pattern. The electrons that are contained in the sharp peak have not traveled to great depths into the specimen, thus BEKP is a technique that samples a relatively thin surface layer. Lower accelerating voltages will result in a signal that is more highly localized to the surface of the specimen. The electrons that have experienced larger energy losses contribute to the overall background intensity in the patterns.

The diffracted electrons form cones of intensity. The cone axis is normal to the crystal planes that satisfied the Bragg condition and the cone semi-angle is 90° minus the Bragg angle. Since the Bragg angle is relatively small (about 3°) the cones are very shallow (12). The diffracted cones are then detected with an appropriate detector. When the cone of intensity intersects a planar detector surface, a conic section is produced. However, since the cone angle is large, the conic sections are nearly straight lines and appear curved only at low beam energies where the Bragg angle is larger.

Information Available From BEKP

Figure 2 shows a BEKP obtained from a metallographically polished Ni sample that was recorded using an accelerating voltage of 20 kV and a slow scan CCD camera. The pattern consists of a large number of parallel lines. Each line pair is the result of diffraction from the front and back of a particular plane in the crystal.

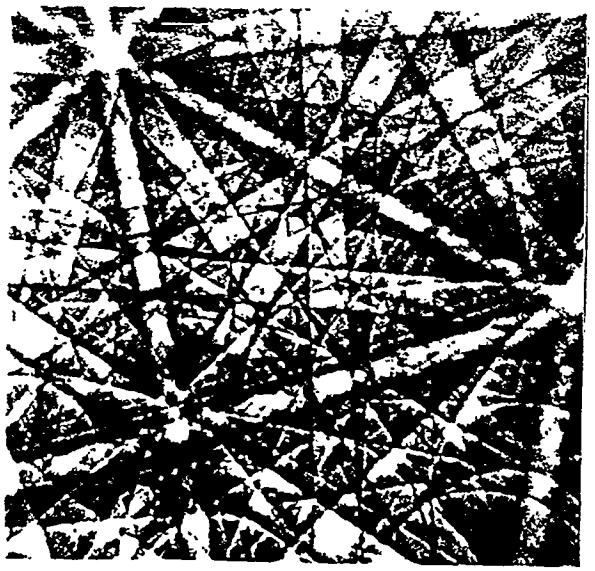

Fig. 2 BEKP of metallographically prepared Ni recorded at 20 kV.

The angular width between each line pair is proportional to the interplanar spacing that gives rise to the line pair. The pattern also contains a number of prominent areas where the pairs of lines intersect. These intersections are zone axes and the angle between the various zone axes is indicative of the samples crystal structure.

BEKP's can be obtained for a range of accelerating voltages (and therefore electron wavelengths). Figure 3 a and b shows patterns obtained from Si at 40 and 10 kV. The positions of the zone axes remain fixed as the angular relationship between zone axes is determined by the crystal structure of the sample and not the beam voltage. The width of the line pairs vary with the accelerating voltage as described by Bragg's Law. As the wavelength of the electrons increases (lower accelerating voltages) the Bragg angle increases. Thus the line pairs will have a larger angular spacing between them. This is apparent when Figure 3a is compared to Figure 3b. The increased curvature of the line pairs at lower accelerating voltages is also apparent in Figure 3b along with the reduced definition of the lines at the lower operating voltage due to the larger energy loss suffered by the electrons.

It is fairly easy to calculate the orientation of the specimen from a single pattern (13,14). This is the basis of the technique of orientation imaging microscopy (OIM) where the orientation of a microstructure is mapped by obtaining patterns at each point in an array of points on the sample surface and then using orientation differences between the patterns to delineate microstructural features (14-17).

Collection of Backscattered Electron Kikuchi Patterns

BEKPs can be successfully collected using photographic film, video rate camera technology or slow-scan CCD technology. Although high quality patterns can be collected on photographic film, film suffers from the disadvantage that the collected image can be viewed only after the film is developed. BEKP's have been collected with video rate cameras. In this arrangement the diffracted electrons from the sample strike a scintillator that converts the electrons to light. The scintillator is then viewed with a video rate low light level camera to produce an image on a TV or computer screen. Patterns collected in this manner are suitable for the determination of sample orientation, but are not of sufficiently high quality for phase identification.

In order to overcome the disadvantages of photographic film and video rate recording of the patterns, a camera was developed based on CCD technology. This camera consists of a thin yttrium aluminum garnet (YAG) scintillator that is fiber optically coupled to a scientific-grade thermoelectrically-cooled slow-scan CCD. A CCD with 1024X1024 pixels was chosen for this application to achieve high accuracy in the measurement of the recorded BEKP. In order to achieve a large collection angle the CCD, 2.54 cm X 2.54 cm, was coupled to the scintillator through a 2.5:1 fiber optic reducing bundle. This detector configuration permits high quality patterns to be recorded using exposures of 1 to 10 seconds (11). The actual exposure depends on the specimen (atomic number) and the electron optical conditions (accelerating voltage and beam current).

The CCD is a good replacement for photographic film recording of BEKP's. Typically, high quality CCDs have a higher dynamic range than photographic film, but the resolution of the CCD still cannot approach the resolution of photographic film (18,19). However, for images collected at a resolution of 1024X1024, it is difficult for the unaided eye to resolve the individual pixels. For phase identification using BEKP in the SEM, CCD detectors are superior to film due to the high dynamic range of the CCD and their adequate resolution and the immediate availability of the image for analysis (19).

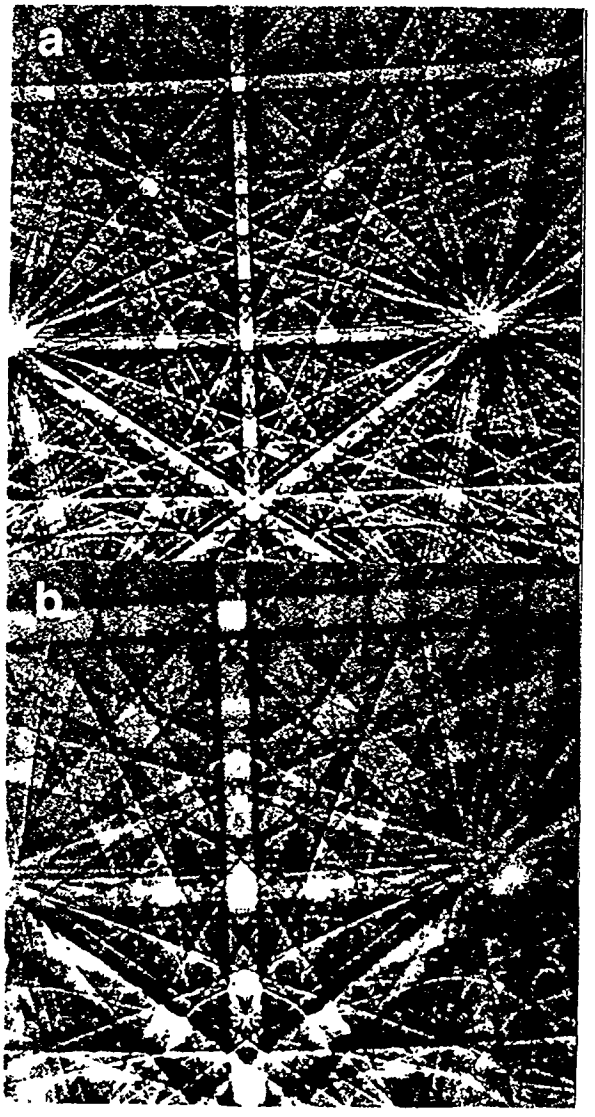

Fig. 3. BEKP of Si obtained in the SEM using CCD camera. a) 40 kV, b) 10 kV.

The patterns obtained are improved significantly by an image processing procedure called flat fielding (18). The raw patterns collected with the CCD consist of relatively weak but detailed crystallographic information superimposed on a slowly changing background intensity and image artifacts related to the fiber optic bundle and the scintillator. Once a raw image has been recorded a second image (the flat field image) is recorded that contains everything but the crystallographic information. This image may be obtained by scanning the beam over a number of crystals while collecting a pattern or by recording patterns from very fine grained materials. The image artifacts and the slowly varying background component can be removed by normalizing the raw image containing the crystallographic information with the flat field image. This procedure has the added advantage of increased contrast in the processed patterns. An example of the flat fielding procedure is shown in Figure 4 a and b.

The accurate determination of crystallographic parameters from BEKPs requires that the camera system be carefully calibrated (15). The two parameters that require calibration are the pattern center and the specimen to detector distance. The pattern center is defined as the projection of the beam impact point onto the scintillator. There are a number of ways to calibrate the pattern center. We have found that one of the most accurate and simple ways to accomplish this is to record patterns from the same crystal at two different scintillator to specimen distances (11). The crystallographic zones move along radial lines that project out from the pattern center. It is quite simple to plot the positions of the zones as they move to determine the pattern center. This technique has been used to determine the pattern center to within one or two pixels. The CCD camera has been calibrated using this procedure and has been found to be extremely stable with time. Once the pattern center is accurately known the specimen to detector distance can be easily determined from a known specimen. Table 1 shows the measured angles between zones in Figure 3a and compares the measured values with values calculated from the crystal structure.

Table I. Comparison of measured interzonal angles with actual angles for Si

Angle between	Measured (°)	Actual (°)
[001] - [111]	54.81	54.7
[001] - [011]	44.93	45.0
[011] - [112]	29.94	30.0

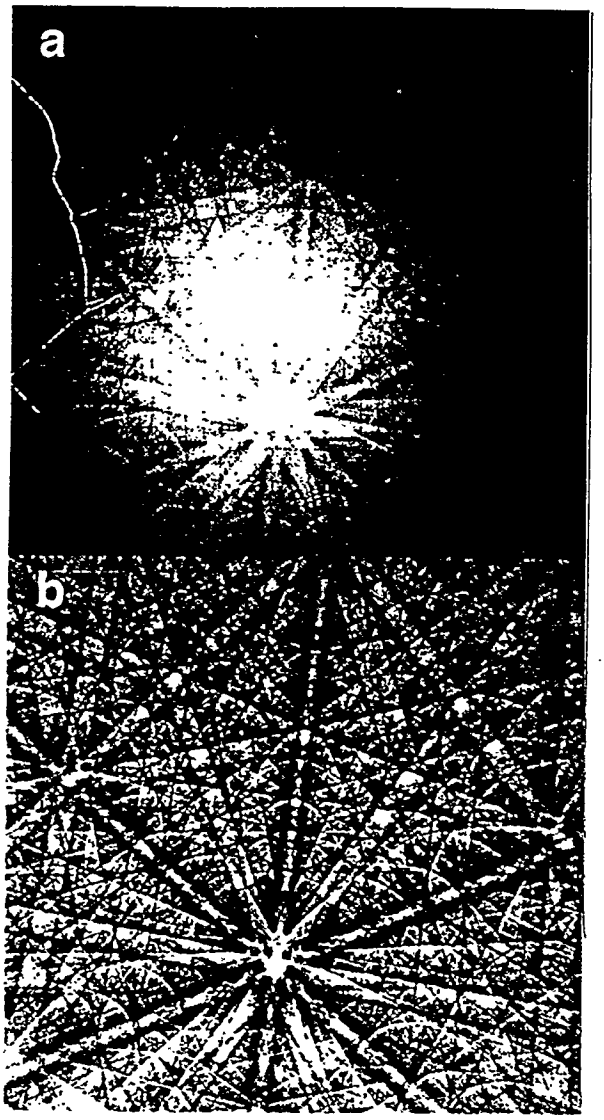

Fig. 4 Flat fielding procedure can greatly increase contrast and quality of BEKP images. a) raw image before flat fielding b) image after flat fielding.

Procedure for Phase Identification using BEKP

Phase identification with BEKP in the SEM has previously been accomplished by recording patterns on film. On-line phase identification has not been possible due to the necessity to expose and develop the photographic film. The CCD detector system eliminates this problem, as the patterns are immediately available for viewing and analysis and are of similar quality to those obtained on photographic film. Phase identification is achieved in the following manner.

First an area of interest is located on the tilted specimen using the appropriate imaging signal (backscattered or secondary electrons). A BEKP is then collected from the

feature of interest using a stationary beam in the same way that x-ray information is obtained. A flat field image is then obtained and used to flat field the raw image data as has been described previously. Compositional data is also obtained from the feature of interest as this information is used to limit the number of possible candidate materials that could produce the BEKP.

The next step in phase identification using BEKP is to determine the angles between the various zone axes present in the image. Candidate crystal structures, consistent with the compositional information obtained from the unknown, are selected from the literature. The measured interzonal angles are then compared with those calculated from the candidate crystal structure. Quite often these angles and the compositional information are sufficient to unequivocally identify the unknown crystalline phase. Once a possible match is found, the pattern is simulated in the correct orientation. The simulation includes the effect of structure factors and calculates the relative intensity for each reflection. The simulated pattern is compared to the experimentally obtained pattern and if the agreement between the experimental and the simulated pattern is good, then an identification is assumed to have been accomplished.

It should be noted that in a vast majority of cases there is no need to make use of the interplanar spacings that can be measured from the BEKPs. Cubic materials present the most difficulty in using the approach described above becuase the interzonal angles do not vary with the lattice spacing of the crystal. As the symmetry of the crystal decreases the angles between the zone axes in the pattern becomes more diagnostic. Fortunately, it is possible to measure the interplanar spacings from a BEKP. This is done by measuring the angle between the pair of lines that produce the Kikuchi band and converting this angle to a interplanar spacing (14). This data can then be used as a further condition for identifying the unknown phase of interest and is particularly useful for cubic crystal structures.

Examples of Phase Identification

Identification of Laves Phase in Welds

During the simulated welding of an Fe-Co-Ni-Cr-Nb alloy a second phase was observed in metallographically prepared sections. Figure 5 is a backscattered electron image of the simulated weld that shows the precipitates that image brighter than the matrix phase. EDS x-ray analysis in the SEM demonstrated that the second phase was rich in Fe and Nb.

BEKPs of the bright imaging phase were obtained from a metallographically polished, but not etched sample. The SEM was operated at 30 kv with a beam current of 1-2 nA. Figure 6 shows an example of the BEKP from the bright precipitates in the simulated weld. A survey of the literature showed that there were a number of phases that contain Fe and Nb. Possible Nb-Fe phases were NbFe, Fe_2Nb and Fe_7Nb_6 (20). Interzonal angles observed in the experimental patterns were measured and compared with the calculated values for the above three compounds. Good agreement was found between the interzonal angles for Fe_2Nb and the experimentally measured interzonal angles. Patterns for Fe_2Nb were simulated, including the effects of structure factors, and the simulation was compared with the experimental patterns. Figure 7 is a BEKP simulation for Fe_2Nb calculated using the same microscope parameters as those used for collecting the BEKP from the unknown bright phase. As can be seen from comparison of Figure 6 and Figure 7 the agreement is excellent. Thus, the bright phase was identified as Fe_2Nb, a Laves phase that is hexagonal (a=.4837 nm and c=.7884 nm).

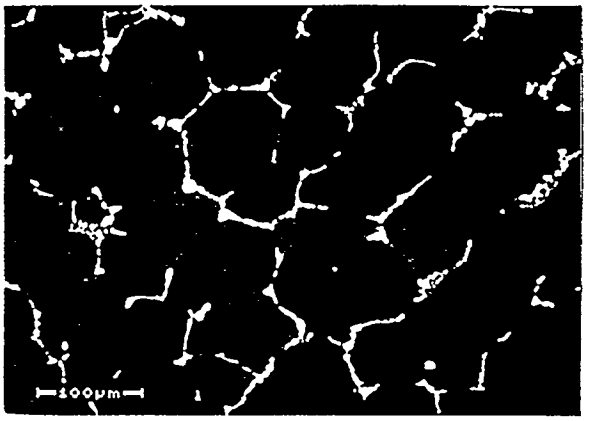

Fig. 5. Backscattered electron image of weld simulation in Fe-Co-Ni-Cr-Nb alloy.

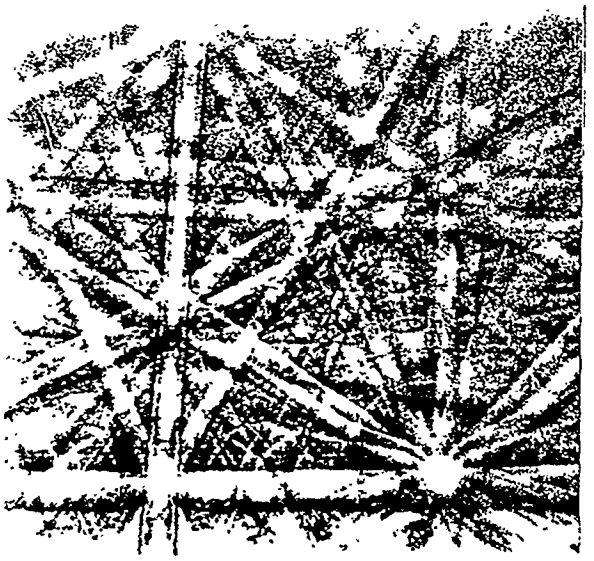

Fig. 6. BEKP obtained from the bright phase shown in Figure 5.

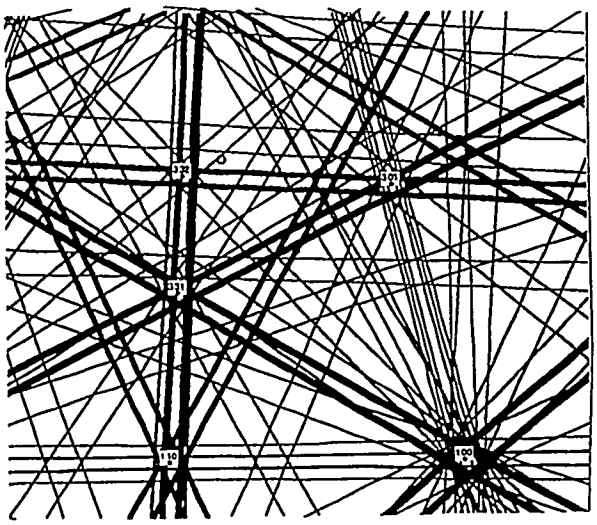

Fig. 7 Simulated BEKP of Fe_2Nb that demonstrates excellent agreement with Figure 6.

Fig. 8 Bright field TEM micrograph of the bright phase shown in Figure 5.

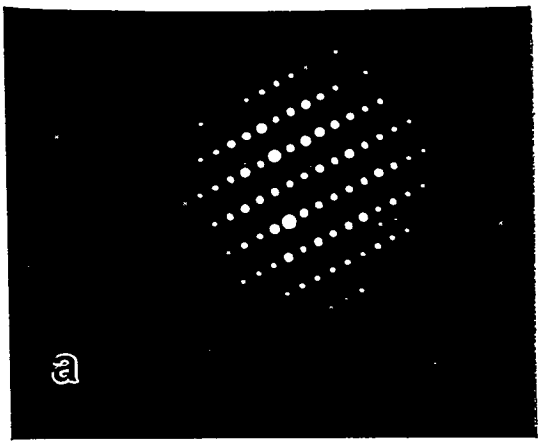

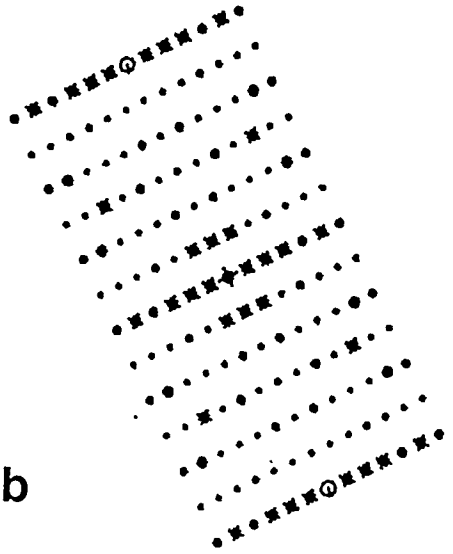

Fig. 9 Experimental and simulated SAED patterns from the Laves phase (Fe_2Nb) shown in Figure 8. a) experimental, b) simulated [2 -1 -1 0] zone.

In order to verify and demonstrate the correct identification of the bright phase as Fe_2Nb, selected area electron diffraction (SAED) was performed in the transmission electron microscope. SAED in the TEM requires that thin foil samples be produced from the bulk weld material. This can be a tedious and time intensive procedure and is particularly so when samples with large second phase precipitates are to be produced. In the case of the Fe-Co-Ni-Cr-Nb alloy electropolishing was used to produce electron transparent specimens for SAED analysis. This demonstrates one of the main advantages of BEKP for phase identification which is the lack of time consuming specimen preparation. Figure 8 is a TEM bright field micrograph of the bright phase shown in Figure 5. In order to obtain good indexable SAED patterns in the TEM it is necessary to tilt the specimen carefully to obtain a zone axis pattern. The limited angular view of SAED in TEM requires that the specimen be tilted to a variety of zone axes so that the phase may be identified. Figure 9a is a SAED pattern of the phase shown in Figure 8. Figure 9b shows a simulation of the SAED shown in Figure 9a. In order for a complete analysis a number of patterns were collected and indexed. The SAED analysis in the TEM demonstrated that the second phase in the simulated weld was indeed Fe_2Nb confirming the conclusions of the BEKP analysis. The limited angular view provided by SAED in the TEM is a distinct disadvantage of the technique that requires multiple patterns to identifiy a phase. The large angular view provided by BEKP permits the collection of data from a large portion of the stereographic triangle in only one

Fig. 10. Secondary electron image of the crystals on the PZT thin film.

exposure thus obviating the need to tilt to obtain different patterns.

Identification of Crystals on PZT Thin Films

The previous example demonstrate the applicability of phase identification using BEKP to metallographically prepared specimens. This example demonstrates that the technique can also be used on rough surfaces. In this example BEKP was used to identify crystals that had formed during the thin film processing of lead zirconium titanate (PZT) thin films. The processing involved the deposition of thin films of RuO_2 onto Si wafers followed by the deposition of the PZT thin film. After deposition of the PZT, crystals on the surfaces of the processed wafers were noted. Figure 10 is a SEM photograph of the crystals on the PZT films. The crystals were on the order of 1-2 μm in size and were distributed across the wafer surface. In this case it would be quite difficult to prepare suitable samples for TEM analysis so identification was attempted using BEKP.

Figure 11 is a BEKP obtained from a crystal shown in Figure 10. The pattern is very clear and well defined, even though it was obtained from a non-flat specimen that had been coated with carbon for conductivity. Qualitative EDS analysis of the crystals showed them to contain Pb, Ru, and possibly O. The interzonal angles were measured and are shown in Table 2 and indicate that the crystals structure was cubic, i.e. that the three lattice parameters are equal and at 90° to each other. Table 2 also shows a comparison of the experimental values with those calculated for a cubic crystal structure. Examination of the literature indicated that there were no oxides of Pb or Ru that were cubic, however there is a cubic pyrochlore phase $Pb_2Ru_2O_{6.5}$ that had been reported. It is important to point out that the interzonal angles

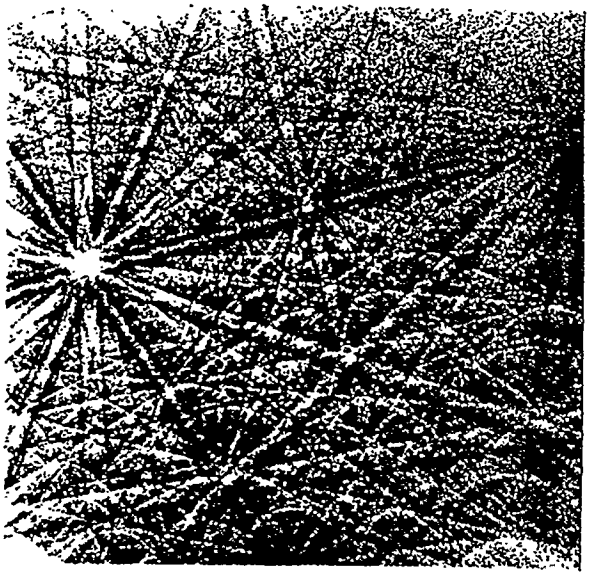

Fig. 11. BEKP obtained from a crystal shown in Figure 10. The pattern was obtained at 40 kv.

Table II. Comparison of interzonal angles from BEKP of crystals on PZT with angles calculated for cubic compounds

Angle Between	Measured (°)±0.3°	Computed (°)
[110] - [310]	26.6	26.6
[110] - [211]	29.9	30.0
[110] - [121]	30.4	30.0
[110] - [111]	35.2	35.26
[111] - [121]	19.7	19.5
[100] - [110]	44.5	45.0

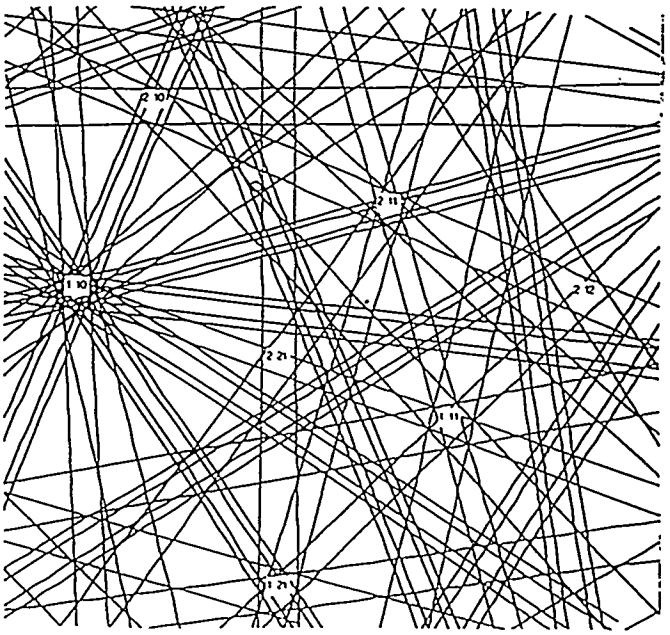

Fig. 12 Simulated pattern of $Pb_2Ru_2O_{6.5}$ that shows excellent agreement with the experimental pattern shown in Figure 11.

indicate only that the crystal structure is cubic, all cubic materials will have the same interzonal angles. Unequivocal identification required that the d-spacing be measured and compared with those for $Pb_2Ru_2O_{6.5}$. Table 3 shows the d-spacings measured from the pattern shown in Figure 11. The measured d-spacings are in good agreement with the reported values for $Pb_2Ru_2O_{6.5}$. Although, in this case the agreement is quite good, further development is needed to routinely extract accurate d-spacing measurement from these patterns.

Table III. Comparison of measured and computed d-spacings for $Pb_2Ru_2O_{6.5}$

Plane (hkl)	Measured d (nm)	Computed d(nm) a=b=c=1.025 nm
(222)	0.30±0.02	0.2959
(400)	0.25±0.01	0.2563
(440)	0.18±0.01	0.1812
(220)	0.15±0.01	0.1546

The final step in the identification of the crystals as $Pb_2Ru_2O_{6.5}$ is to simulate the BEKP. Figure 12 shows the simulation of the pattern. Comparison of this simulation with the experimental pattern shown in Figure 11 demonstrates excellent agreement and thus the crystals that grew on the PZT film were identified as $Pb_2Ru_2O_{6.5}$.

Summary

The combination of BEKP and EDS now permits the unequivocal identification of micron sized areas in the SEM. The ability to obtain high quality BEKPs without the use of photographic film enables the patterns to be analyzed rapidly. No other technique can as quickly and accurately provide the identification of the crystallography of micron-size areas of a specimen. In this paper we have described the origin of and the information contained in these patterns. This paper has demonstrated the crystallographic identification using BEKP of unknown phases in metallographically prepared samples and of unprepared surfaces. Although unequivocal identification is not yet possible in the general case, the combination of diffraction information from BEKP and compositional information from EDS is a powerful tool for materials characterization.

Acknowledgments

The authors would like to thank Dr. B. A. Tuttle for supplying the specimens of PZT and Dr. C. V. Robino for the specimens of the simulated weld. The authors would also like to thank Dr. T. J. Headley for his careful review of this paper. This work was supported by the U.S. Department of Energy under contract #DE-AC04-94AL85000.

References

1 Alam, M. N., M. Blackman and D. W. Pashley, Proc. Roy. Soc., 221, 224 (1954).
2 Venables, J. A. and C. J. Harland, Phil. Mag., 27,1193 (1973).
3 Venables, J. A. and R. Bin-Jaya, Phil. Mag., 35,1317 (1977).
4 Dingley, D. J. SEM, IV, 273 (1981).
5 Dingley, D. J. SEM, II, 569 (1984.
6 Dingley, D. J. and K. Baba-Kishi, SEM, II,383 (1986)
7 Baba-Kishi, K. Z. and D. J. Dingley, Scanning, 11, 305 (1989).
8 Baba-Kishi, K. Z. and D. J. Dingley, J. Appl. Cryst., 22, 89 (1989).
9 Baba-Kishi, K. Z. Ultramicroscopy, 36, 355 (1991).
10 Baba-Kishi, K. Z. J. Appl. Cryst., 24, 38 (1991).
11 Michael, J. R. and R. P. Goehner, MSA Bulletin, 23, 168 (1993).
12 L. Reimer, "Scanning Electron Microscopy," p 313,Springer-Verlag, New York (1985).
13 Harland, C. J. , P. Akhter, and J. A. Venables, J. Phys. E: Sci. Instrum., 14, 175 (1981).
14 Wright, S. I. and B. L. Adams, Metall. Trans. A., 23, 759 (1992).
15 Dingley, D. J. and V. J. Randle, Mater. Sci.,27, 4545 (1992).
16 Adams, B. L., S. I. Wright, and K. Kunze, Metall. Trans. A.,24A, 819 (1993).
17 Wright, S. I., B. L. Adams, and K. Kunze, Mat. Sci and Eng., A160, 229 (1993).
18 Kujawa, S. and D. Krahl, Ultramicroscopy, 46, 395 (1992).
19 Janesick, J. R., T. Elliot, S. Collins, M. M. Blouke and J. Freeman, Optical Engineering, 26, 692 (1987).
20 P. Villars, and L. D. Calvert, "Pearson's Handbook of Crystallographic Data," p 3303, ASM International. Metals Park, OH (1991).

DISCLAIMER